

Gravimetric detection of sinkhole hazard at abandoned coal mine Čáry (Slovakia) using Growth inversion – preliminary results

Jozef BÓDI^{1,2,3} , Peter VAJDA^{2,*} , Pavol ZAHOREC² ,
Roman PAŠTEKA³ , Juraj PAPČO⁴ , René PUTIŠKA³ ,
Bibiana BRIXOVÁ³ , José FERNÁNDEZ¹ 

¹ Institute of Geosciences, CSIC-UCM, Madrid, Spain

² Earth Science Institute, Slovak Academy of Sciences,
Dúbravská cesta 9, P.O. Box 106, SK-840 05, Bratislava, Slovakia

³ Dept. Engineering Geology, Hydrogeology and Applied Geophysics,
Comenius University in Bratislava, Slovakia

⁴ Dept. Global Geodesy and Geoinformatics, Slovak University of Technology,
Bratislava, Slovakia

Abstract: Microgravimetry has been used in near surface investigations for detecting cavities. It has already proven its success in revealing unknown crypts and tombs in archaeological prospection. It was involved in searching for new cave spaces in karst. It was also employed in detecting void spaces in shallow-mining areas to mitigate sinkhole hazard. In our study we focus on the applicability, benefits and limitations of using the 3D Growth inversion approach for inverting the high-resolution high-precision micro-gravity data observed in undermined areas with the purpose of detecting shallow void space that could lead to sinkhole development, slow surface subsidence or collapses. Growth inversion has several free, user-specified inversion parameters that shape the Growth solution. Our case study presented here is related to sinkhole hazard due to abandoned shallow brown-coal mining under fields with agricultural activities. We pay attention to tuning these parameters for specific needs of cavity detection in terms of long and narrow shallow mining shafts.

Key words: near surface geophysics, 3D microgravimetry, inverse problem, subsurface voids, growing source bodies, sinkhole hazard

1. Introduction

In this work we focus on microgravimetric detection of near surface cavities that can pose hazard to human lives or infrastructure, based on the

*corresponding author, e-mail: Peter.Vajda@savba.sk; mobile: +421 948 044 717

application of the Growth inversion approach. The input gravity data, the residual complete Bouguer anomaly (local anomaly), often abbreviated as RBA or LBA, in such detection typically represent signals at the level of several or several tens of μGal ($1 \mu\text{Gal} = 10 \text{ nm/s}^2$). The purely gravimetric solutions, including the Growth models, are highly ambiguous. That means that several diverse solutions can nearly equally well satisfy (fit) the observed gravity data. Discriminating among these solutions, in search of the most realistic one, can be done only by employing constraints in terms of results from other geophysical methods, or information stemming from geologic, or other independent cognition or assumptions. The data noise translates into model noise, while the model uncertainty grows with depth. Therefore high-resolution, sufficient coverage, high-accuracy micro-gravity data are a pre-requisite for successful detection of shallow cavities or structural studies of the near-surface.

Despite other approaches can be used to interpret microgravimetric data, here we focus only on the applicability of the Growth inversion. It is based on dividing the subsurface into a fixed-geometry set of elements (cells), namely right-rectangular prisms, seeking only the constant density contrast of each cell. The subsurface is explored, the cells are probed and filled in an iterative adjustment process. The coalesced filled cells form the model source bodies upon completion of this iterative growth process. The Growth inversion methodology is described in section 2.

The Growth inversion for near-surface microgravimetric applications has been first tested by means of two case studies from the realm of archaeological prospection and sinkhole hazard detection (*Vajda et al., 2024*). The first case study was devoted to detection of crypts in the St. Nicolas basilica of the Trnava town in SW Slovakia. The second focused on detection of shafts in an abandoned coal mine of Wolfsberg (Austria) that pose sinkhole hazard. In both case studies the Growth inversion appeared as promising.

Next, we continued assessing the benefits and limitations of the Growth approach in microgravimetric void-space detection by means of additional three case studies (*Bódi et al., 2025*). The first case study dealt with detection of crypts in the St. George church of the homonymous town (Svätý Jur) near Bratislava, the capital of Slovakia. The second dealt with sinkhole hazard and surface collapses above the coal mine Koš in the Upper Nitra valley of central Slovakia. The third focused on sinkhole hazard in a

densely populated urban area in the Pincesor quarters of the town Senec (SW Slovakia) threatened by an extensive complex of only partially known cellars. These three case studies indicated the pros and cons of using the Growth inversion approach to interpret shallow void spaces in near-surface microgravimetry.

Here we continue in this investigative effort. In section 3 we present a case history devoted to identification of shallow void space that may be associated with sinkhole hazard. The suspect shallow cavities are mining shafts related to abandoned coal mining in Čáry in the Slovak part of the Vienna Basin (SW Slovakia).

2. Growth inversion in 3D microgravimetry

To avoid repetition, we do not give here a complete or comprehensive description of the Growth inversion methodology. Instead, we refer the reader to *Bódi et al. (2025)* for a brief overview of the features of the inversion approach, or to *Vajda et al. (2024)* for a comprehensive phenomenological description of the Growth inversion, or eventually to *Camacho et al. (2021a, 2021b, 2024)* for a complete explanation of this inversion approach including mathematical apparatus.

For our investigations we use two implementations of the Growth inversion, GROWTH-dg (*Camacho et al., 2021b*) for seeking homogeneous solutions (source bodies), and GROWTH-23 (*Camacho et al., 2024*) for heterogeneous solutions. The advantage of the GROWTH-dg tool dwells in the option to seek homogeneous source bodies of pre-specified density contrasts, which suits well the search for cavities.

In the Growth inversion approach the volumetric domain below the topographic surface, on which the gravity data are given, is divided into cells, namely right-rectangular prisms. These are, during an iterative adjustment process, gradually populated with pre-defined density contrasts, which facilitates the growth of source bodies of the model. When adequate (controlled by a pre-defined factor) fit to the gravity data is reached, the process terminates, creating the final model of the growth process. This adjustment procedure must be regularized. The regularization is mediated by minimizing the total mass of the model, which implies a smoother and more compact model. The weight between minimizing the data misfit and mini-

mizing the total model mass is governed by the so-called balance factor (λ). The value of λ is set by the user prior to running the inversion and imposes the character of the source bodies of the solution as well as the level of data misfit.

The balance factor is the most essential inversion parameter of the Growth approach. Small values of λ produce overfitting models, in which the data noise is translated into model noise in terms of scattered isolated filled prisms or ripped shapes of source bodies. High values of λ result in over-regularized (over-compacted) models with less source bodies of smaller sizes and rounder shapes that may be falsely vertically shifted towards greater depth. Growth offers an automatically determined default value for λ prior to the growth process execution. This value can be changed by the user. The proper setting of the λ value is assisted by the autocorrelation function displayed on the running screen upon executing Growth. A trial-and-error approach of repeated inversions should be exercised aiming at reaching a nearly null value of autocorrelation for zero distance. Observing the character of the resulting model (not too noisy, not too compacted) throughout this approach is helpful, too. Observing the distribution and size of misfit residuals assists this approach also.

Another key concept in the Growth inversion is the density contrast used for the model. The density contrast is not a quantity resulting from the inversion. Rather, it is a free inversion parameter preset by the user prior to running the inversion routine. As such, it has essential impact on the appearance of the model.

GROWTH-dg (*Camacho et al., 2021b*) can seek homogeneous source bodies, of (both positive and negative) preselected (by the user) density contrast, submerged in homogeneous background. Therefore, it is particularly suitable for seeking unknown cavities, as they have a known negative constant density contrast, dictated by the density of the rock environment in the shallow subsurface (relative to the density of air). GROWTH-23 (*Camacho et al., 2024*) allows only heterogeneous models. GROWTH-23 can work with both homogeneous and stratified (with stepwise downwards increasing density) background medium. For inversions with homogeneous background, the program adopts four levels of density contrast for the heterogeneous source bodies, while for stratified density (of the background and of the model) it adopts 30 levels of density contrast. In near-surface

microgravimetric applications we focus on shallow subsurface, hence we use only homogeneous background medium.

In GROWTH-23, the user can no longer specify the value of the target average density contrast and the number of density levels. This is done automatically. Instead, GROWTH-23 uses the pre-set amount of filled cells (in %) out of all subsurface cells as the end condition for the iterative inversion process. The default % value can be changed by the user prior to running the inversion process. The application of GROWTH-23 to microgravity data (local gravity anomalies, residual micro-CBA data) is somewhat similar to inverting gravity changes (4D microgravity data), since seeking shallow cavities implies a small number of source bodies, i.e., a low % value of filled cells. This inversion parameter (%) is also a key parameter in the Growth process, as it implies the values of the final model density contrasts. Therefore, the user should sensibly vary this value in a trial-and-error approach of repeated inversion runs (along with sensibly varying the λ value), while observing the character of the resulting model. A small size model (with a small relative number of filled cells) will imply larger density contrasts, while a very large model (with high percentage of filled cells) will result in smaller density contrasts. By experimenting with the end value during repeated inversion runs, the user can target the final model to a desired or expected average density contrast solution.

Handling the model density contrast in the Growth inversion is an important concept to be understood by the user. The density contrast of the model (solution) is not a unique product of the inversion. The density contrast of the Growth solution remains ambiguous. Several models with diverse density contrasts may be obtained which produce a fair, reasonable fit to the gravity data (acceptable misfit residuals in terms of r.m.s.). Models with smaller density contrasts will contain bulkier (more voluminous) source bodies and vice versa. It is not possible to discriminate among the models purely on basis of the gravity data. To judge which models are more realistic, external constraining information must be employed. For instance, if we seek underground cavities, we know that their density contrast will be negative and of the value defined by the density of air and the rock environment in which they reside.

If outliers (blunders) are suspected to possibly be present in the input gravity data, the data reweighting functionality should be enabled, sup-

pressing or eliminating the extreme residuals (outlier data) contribution into the adjustment throughout the iterative growth process. This iterative reweighting is controlled by the “blunder value” parameter. The cut-off values (higher than cut-off values mean weak or no reweighting) are set as 3.8 for CBA data and 2.2 for gravity changes, which may also well be the case of local microgravity anomalies. Anyhow, blunders are seldom present in micro-gravity data sets. Hence this Growth functionality will be rarely used in microgravimetric studies.

The feature of GROWTH-23 for stratified background medium with step-wise linear downward increasing density, mediated by the flattening coefficient, is unlikely to be applied in near-surface microgravity inversion. A pre-set zero value of the flattening factor means no stratification (homogeneous background). This option is proper for inverting microgravity data, which seeks shallow source bodies in likely homogeneous background.

GROWTH-23 contains also a feature for forcing the solution into shallower depths. For inversion of microgravity data, the preferred value for the upward forcing parameter is in most cases zero, unless the data are due to a flat-like shallow or surface-bound source body. The value of the upward-forcing parameter should be used with caution or varied sensibly in a trial-and-error process of repeated inversion runs. External constraints must be used wherever available, such as borehole data.

In addition, Growth (both GROWTH-dg and GROWTH-23) can co-adjust, during the iterative growth process, also an additional offset or linear trend in the input gravity data. In some microgravimetric applications this functionality may turn out very beneficial, as we learnt in our case study devoted to a cellar in complex urban settings (Bódi et al., 2025). In other cases, it may turn out counter-productive.

Upon completion of the iterative inversion procedure, a final model is obtained. It is graphically displayed on the screen as several horizontal slices (at automatically chosen depths) and several W–E vertical sections (at automatically chosen northings). In addition, two ASCII output files are generated: “Mod.txt” listing the values of the used inversion parameters, and the information about the populated cells; and “Fil.txt” listing the observed, modelled and residual values, including offset/trend. The set of filled cells listed in Mod.txt can be used to import the information into visualization software of third parties to present the model in 3D indepen-

dently.

The specifics of applying Growth to microgravity data concern the small size of the data spacing and the use of coordinates different from UTM. How to deal with these issues was discussed in section 3 of *Bódi et al. (2025)*.

3. Sinkhole hazard in undermined area – abandoned coal mine at Čáry (SW Slovakia)

This case study is situated in a recently abandoned mining area of the Čáry Mine at the NE part of the Neogene Vienna Basin, western Slovakia. The mined coal bed in the investigated area was very shallow, mainly at 10 m below surface, at places reaching 20 m. The overburden consists of sands and clays. This site was mined by walling for collapse (the long-wall method) using complex mechanized reinforcement, in which no pillars remain. The thickness of the lignite coal seam varied from 3.4 to 6.5 m, of which 3.6 m was mined. Some of the original access corridors have not yet completely collapsed, probably due to residual roof support, and are now causing the occurrence of intermittent, ongoing surface subsidence/collapse. Mining in the investigated section took place in the 1990s (*Čangel, 2019; Zahorec et al., 2021*).

The gravity survey (*Zahorec et al., 2021*) at this site was prompted by the recurrent formation of sinkholes in a relatively small, linear area in 2016–2018 (see Fig. 1). These sinkholes are probably mainly associated with the second longitudinal access corridor, further away from the mine buildings (denoted Ch116.1 in Fig. 1), in Fig. 2 marked by the two black arrows labelled “2”), about 400 m long, which had not fully collapsed yet, likely due to residual roof support. The other longitudinal access corridor, closer to the mine buildings is labelled “1”. The crosswise corridor connecting the two longitudinal corridors in the NW part of the data area is labelled “3”. Average elevation of the surface relief in the data area is 163 m a.s.l.

Currently, sinkholes occur only at the SE part of this corridor. The purpose of the survey was to verify whether there is a risk of collapse in other parts of this corridor. Microgravity measurements over the area were carried out along profiles, perpendicular to the longitudinal corridor, with a measurement step of 4 m and profile spacing of 20 m on average. Residual complete Bouguer anomalies (residual CBA data) were compiled, using a



Fig. 1. The map showing the mining site plan (after Čangel, 2019, Fig. 5). Exploratory corridors are shown in light yellow framed by solid black lines. Bold black dots are boreholes. Red dots mark sinkholes developed in 2016–2018. The yellow-hatched area is protected to prevent the entry of agricultural machines due to hazard of sinking.

reference topographic density of 2200 kg/m^3 , with accuracy estimated at $14 \mu\text{Gal}$ (r.m.s.). Gravity points were positioned (easting and northing) in S-JTSK coordinates. The residual CBA data are portrayed in Fig. 2.

The pronounced gravity low in the NW sector is labelled “A”. Only a margin of a similar gravity low, labelled “B” is captured by the data area. The NW sector of the data area terminates by a gravity high (red shades), labelled “C”, of which only a margin is captured by the data area. This gravity high is produced by the change in geology (Čangel, 2019).

We used the residual CBA data of Zahorec et al. (2021), as shown in Fig. 2, in our Growth inversions. We used both the GROWTH-23 tool to obtain heterogeneous solutions and the GROWTH-dg tool to arrive at homogeneous solutions.

First, we sought homogeneous solutions with a density contrast of 2200 kg/m^3 , aimed at seeking cavities, applying GROWTH-dg. We used

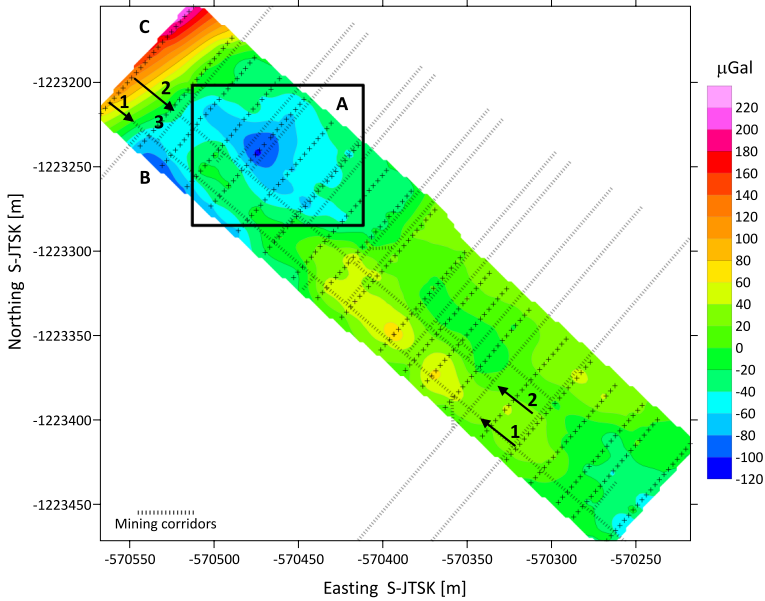


Fig. 2. The residual CBA gravity map of the study area. Crosses mark the gravity points on profiles. Stripe lines mark the position of the exploratory (access) corridors at the average depth of 10 m below surface. The frame indicates the truncated data area used in our Growth inversions focused on the pronounced gravity low in the NW sector (labelled A). For the remaining labels see text.

an average cell size of 8 m, which was the smallest possible. Growth suggested the default value for the balance factor $\lambda = 30$. We tried also lower and higher values. In Figure 3 we present a homogeneous solution with $\Delta\rho = -2200 \text{ kg/m}^3$, $\lambda = 15$, no trend co-adjustment, no reweighting of residuals ($B = 8$), and no depth weighting ($D = 0$). This solution is overfitting (misfit: rms = $7 \mu\text{Gal}$, max = $24 \mu\text{Gal}$).

Although this solution may be polluted by artifacts (model noise) due to overfitting, it seems to indicate small linearly aligned cavities between the surface and the level of the corridors, aligned along access corridor 2, and partly (in the NW part) also along corridor 1, as well as along corridor 3 joining these two at their NW ends (see also the inset in figure B1 in the Supplement). It is the linear alignment parallel with the corridors that raises suspicion that these small cavities are not just arbitrary artifacts. They seem to be related to the corridors. This solution indicates also a

deeper source body (labelled “A”) at the depth of about 40 m below surface, related to the pronounced gravity low (labelled “A” in Fig. 2). This source cannot represent void space, as it could not be reasoned out at this place and such depth. Its position, size and nature will be explored further.

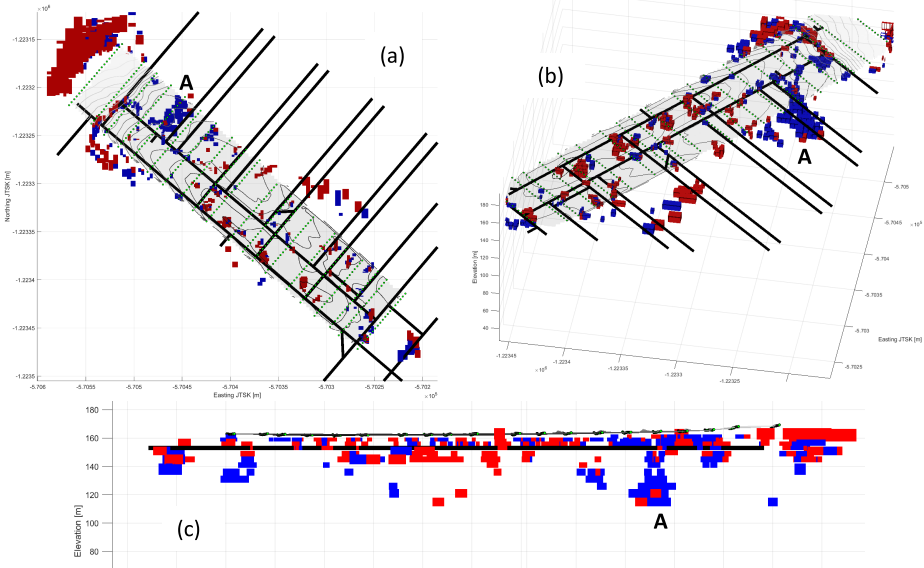


Fig. 3. Overfitting ($\lambda = 15$) homogeneous model ($\Delta\rho = -2200 \text{ kg/m}^3$) with no trend co-adjustment, no residuals reweighting ($B = 8$), and no depth weighting ($D = 0$): (a) top view (az. = 0, el. = 90), (b) 3D view from roughly NE (az. = 100, el. = 40), (c) lateral view from NE (az. = 135, el. = 0). Bold black lines represent access corridors.

In Figure B2 of the Supplement we present a homogeneous solution with $\Delta\rho = -2200 \text{ kg/m}^3$, $\lambda = 30$, no trend co-adjustment, no reweighting of residuals ($B = 8$), and no depth weighting ($D = 0$). This solution is compact with adequate fit (misfit: rms = $15 \mu\text{Gal}$, max = $42 \mu\text{Gal}$). It still seems to indicate some small cavities at or above the level of the corridors in the NW part of the data area. This solution indicates more clearly the deeper source body “A” at the depth of about 40 m below surface. Now the body is more compact compared to the solution of Fig. 3.

We also ran the above two inversions ($\lambda = 15$ and $\lambda = 30$) with the functionality for trend co-adjustment switched on. The co-adjusted trend was insignificant. It had no impact on these two solutions, and would not have any impact on any other Growth solutions for this gravity dataset.

Next, we sought homogeneous solutions with a density contrast of 300 kg/m^3 , aimed at seeking structural geological sources, partly collapsed/filled cavities, or surface collapses filled with tailings, applying GROWTH-dg. Growth suggested the default value for the balance factor $\lambda = 50$. We tried also lower and higher values. In Figure B3 of the Supplement we present a homogeneous solution with $\Delta\rho = -300 \text{ kg/m}^3$, $\lambda = 15$, no trend co-adjustment, no reweighting of residuals ($B = 8$), and no depth weighting ($D = 0$). This solution is a strongly overfitting solution (misfit: r.m.s. = $3 \mu\text{Gal}$, max = $15 \mu\text{Gal}$). The source bodies are relatively inflated compared to the previous solutions. Due to the smaller density contrast, the shallow linearly aligned cavities between the surface and the level of the corridors, associated with access corridor 2, are very clearly pronounced and appear nearly continuous along the entire corridor. Same holds true for the short corridor 3 connecting corridors 1 and 2 at their NW ends. Sporadic shallow cavities appear also along corridor 1. The deep source “A” is present and more voluminous in this solution. Due to the selected density contrast the cavities ought to be interpreted as partly or nearly-fully filled due to collapses.

In Figure 4 we present a homogeneous solution with $\Delta\rho = -300 \text{ kg/m}^3$, $\lambda = 50$, no trend co-adjustment, no reweighting of residuals ($B = 8$), and no depth weighting ($D = 0$). This solution is a tight-fit solution (misfit: rms = $10 \mu\text{Gal}$, max = $28 \mu\text{Gal}$). Some of the cavity space (partly filled) associated with the corridors, mainly along profiles 2 and 3, partly along profile 1, is still present (visible) in this solution (see also inset in Fig. B4 of the Supplement). The deep source body A is rounder in this solution and its bottom boundary reaches a depth of about 60 m below surface.

In Figure B5 of the Supplement we present a homogeneous solution with $\Delta\rho = -300 \text{ kg/m}^3$, $\lambda = 70$, no trend co-adjustment, no reweighting of residuals ($B = 8$), and no depth weighting ($D = 0$). This solution is an adequate-fit compact solution (misfit: rms = $15 \mu\text{Gal}$, max = $42 \mu\text{Gal}$). This solution basically contains only information about the deep source body A and its neighbouring (connected) negative contrast source bodies at the NW end of the data area. As this body cannot be interpreted as void space or back-filled space, the only left-over option is to interpret it as a structural geological source of negative density contrast. However, this hypothesis is pending verification and additional geophysical exploration.

We have not run inversions with iterative residuals reweighting, as the data do not indicate any presence of outliers or bad data, and the data are well spatially correlated. For inversions with enabled depth weighting functionality, we used the GROWTH-23 tool and its upward-forcing feature. With the upward forcing functionality we are going to focus on the deep source body A. We will investigate the possibility of the pronounced gravity low (labelled “A” in Fig. 2) being an expression of a surficial (surface-bound) flat body, interpreted in *Zahorec et al. (2021)* as a back-filled surface collapse.

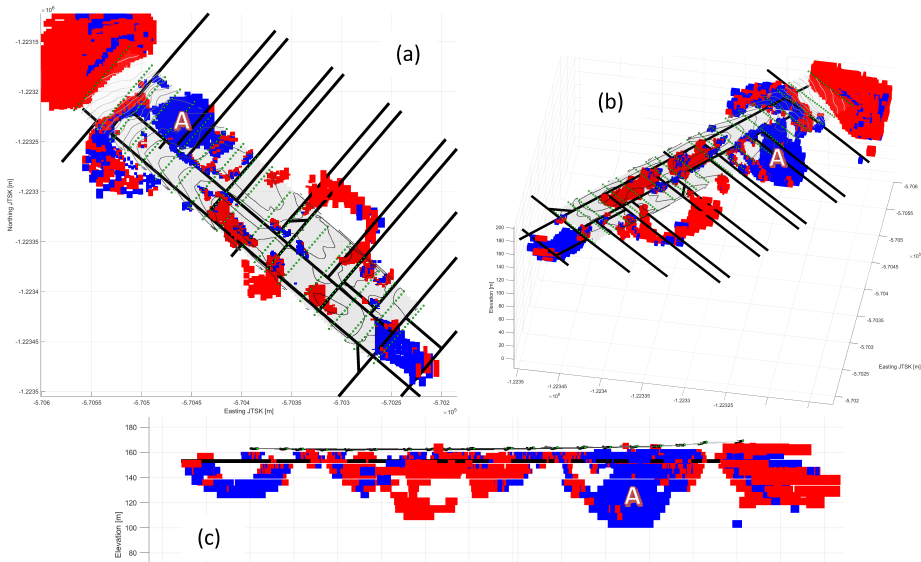


Fig. 4. A tight-fit ($\lambda = 50$) homogeneous model ($\Delta\rho = -300 \text{ kg/m}^3$) with no trend co-adjustment, no residual reweighting ($B = 8$), and no depth weighting ($D = 0$): (a) top view (az. = 0, el. = 90), (b) 3D view from roughly NE (az. = 100, el. = 40), (c) lateral view from NE (az. = 135, el. = 0). Bold black lines represent access corridors.

Next, we investigate heterogeneous solutions with a density contrast around 300 kg/m^3 , aimed at seeking geological sources, partly filled cavities, or surface collapses filled with tailings, applying GROWTH-23. We used again an average cell size of 8 m. Growth suggested the default value for the balance factor $\lambda = 100$, which produced correct fit and solutions thus considered compact. By trial-and-error process we varied the end condition (%) to arrive at the final average density contrast around 300 kg/m^3 . Again,

the engagement of trend co-adjustment had virtually no impact on the solutions. Hence, we present solutions with no trend co-adjustment. Again, as in case of homogeneous solutions, we applied no residuals reweighting, for the same reasons. We applied no flattening ($F = 0$), as no significant downward density increase was expected. We focus on the impact of the upward-forcing functionality on the Growth solution.

In Figure B6 of the Supplement we present a heterogeneous solution with $\% = 5$ (average $\Delta\rho = -280 \text{ kg/m}^3$, $\Delta\rho$ at 4 positive and negative values), $\lambda = 100$, no trend co-adjustment, no reweighting of residuals ($B = 8$), no flattening ($F = 0$), and no depth weighting aka “upward forcing” ($D = 0$). This solution is an adequate-fit, compact solution (misfit: rms = $13 \mu\text{Gal}$, max = $34 \mu\text{Gal}$). This compact heterogeneous solution is very similar to the compact homogeneous solution (cf. Fig. B5 of the Supplement).

In Figure B7 of the Supplement we present a heterogeneous solution with $\% = 5$ (average $\Delta\rho = -267 \text{ kg/m}^3$, $\Delta\rho$ at 4 levels), $\lambda = 100$, no trend co-adjustment, no reweighting of residuals ($B = 8$), no flattening, and weak depth weighting aka “upward forcing” ($D = 5$). This solution is an adequate-fit compact solution (misfit: rms = $15 \mu\text{Gal}$, max = $36 \mu\text{Gal}$). The deep source body “A” is in this solution with weak upward forcing shallower than that in the solution with no upward forcing (cf. Fig. B6 of the Supplement). It spans vertically from a couple of meters below the surface to about 35 m below surface.

In Fig. B8 of the Supplement we present a heterogeneous solution with $\% = 4$ (average $\Delta\rho = -303 \text{ kg/m}^3$, $\Delta\rho$ at 4 levels), $\lambda = 100$, no trend co-adjustment, no reweighting of residuals ($B = 8$), no flattening, and moderate depth weighting aka “upward forcing” ($D = 10$). This solution is an adequate-fit compact solution (misfit: rms = $18 \mu\text{Gal}$, max = $43 \mu\text{Gal}$). The deep source body “A” is in this solution with moderate upward forcing shallower than that in the solution with weak upward forcing. It spans vertically from a couple of meters below the surface to about 28 m below surface. Due to the engaged moderate upward forcing, a pattern of artifacts parallel with the SW–NE trending data profiles gets introduced and becomes dominant.

In Figure 5 we present a heterogeneous solution with $\% = 4$ (average $\Delta\rho = -296 \text{ kg/m}^3$, $\Delta\rho$ at 4 levels), $\lambda = 100$, no trend co-adjustment, no reweighting of residuals ($B = 8$), no flattening, and strong depth weighting

aka “upward forcing” ($D = 30$). This solution has a slightly poorer-fit (misfit: $\text{rms} = 22 \mu\text{Gal}$, $\text{max} = 54 \mu\text{Gal}$).

This solution with strong upward forcing breaks up completely into shallow artifacts placed in-between the data profiles and parallel to them. Even now, the depth-reach of the artifacts related to source body “A” does not get above the horizon of the corridors. This sheds doubts on the possibility that the pronounced gravity low (“A”) is produced solely by a surficial flat thin body of a back-filled surface depression due to surface subsidence as proposed by *Zahorec et al. (2021)*. The vertical extent and nature of body “A” will be the subject of additional exploration by densifying the microgravimetric measurements, as well as by applying additional methods of geophysical exploration.

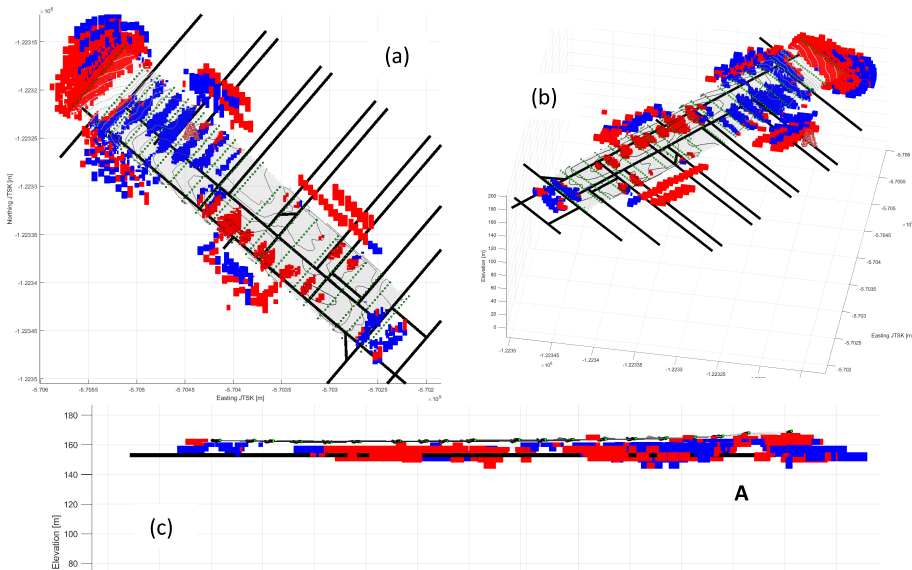


Fig. 5. A compact ($\lambda = 100$) heterogeneous model ($\text{av.}\Delta\rho = -296 \text{ kg/m}^3$) with no trend co-adjustment, no flattening, no residuals reweighting ($B = 8$), and strong depth weighting ($D = 30$): (a) top view (az. = 0, el. = 90), (b) 3D view from roughly NE (az. = 100, el. = 40), (c) lateral view from NE (az. = 135, el. = 0). Bold black lines represent access corridors. Inset in (a) is top view from Growth running screen.

The purpose of Growth solutions with several degrees (“strengths”) of the upward forcing was to see if we can produce a surficial (surface-bound) flat body above the access corridors, responsible for the gravity low “A”,

that could be interpreted in agreement with *Zahorec et al. (2021)* as a back-filled surface depression due to subsidence/collapse. The answer is: Probably not. The reason for doubting the possibility that the pronounced gravity low (“A”) is generated solely by a back-filled surface depression is twofold. First, we were not able to bring the depth reach of source body “A” above the horizon of the corridors even with strong upward forcing ($D = 10$). Second, we studied the Growth-imaging of flat thin surficial bodies by synthetic simulations. Growth without upward forcing images flat thin surficial bodies as empty-bowl-shaped bodies of deeper than original depth reach. Their upper boundary does not adhere to the surface entirely, only at the circumference of the bowl. As the upward forcing becomes stronger, the Growth image of the body attains a shallower depth reach, becomes flatter, and the upper boundary adheres gradually more closely to the surface. Our Growth solutions with increasing strength of the upward forcing on the Čárý data did not follow this pattern. Therefore, we conclude that the gravity low “A” is not caused solely by a surficial depression backfill, as proposed by *Zahorec et al. (2021)*. We plan to verify the existence of the deep source body of negative density contrast (“A”), its vertical position, depth span and its real density contrast, by additional geophysical methods.

The option of depth weighting (upward forcing) introduces another level of ambiguity into the Growth solutions. If there are reasons to apply depth weighting to obtain a more realistic solution, the correct value of the D parameter must be determined by a trial-and-error process, matching the Growth model to borehole data or other applicable independent structural information. The gravity data at Čárý are quite non-uniform, observed on profiles with relatively small step of 4 m, while the spacing between profiles is 20 m on average. The upward forcing (depth weighting), applied to this kind of input data, generates pronounced artifacts at or in-between the data profiles aligned parallel with the profiles. The stronger the depth weighting (the higher the D values), the more is the solution polluted with such shallow artifacts. This pollution even heads towards a checkerboard pattern of artifacts.

We also ran Growth inversions over a data area truncated to the gravity low “A” (see Figs. C5 through C9 in the Supplement).

The spectrum of the obtained fair-fit (and overfitting) Growth models indicates that the sinkhole hazard associated with the two longitudinal cor-

ridors and the corridor connecting their NW ends is still present. This is particularly valid for corridor 1. This is in agreement with the fact that the yellow-hatched area in Fig. 1 is protected by concrete blocks delineating the prohibited access so that agricultural machines are not exposed to the threat of sinking (Čangel, 2019). The sources (of both positive and negative contrast) at or outside the border of the data area are considered solution artifacts, hence are not interpreted.

The second significant feature of our spectrum of admissible Growth solutions is the deep-seated source body of negative density contrast (labelled “A” in Growth models) respective to the pronounced gravity low in the NW sector of the gravimetric survey area (labelled “A” in Fig. 2). This gravity low was 2D modelled by Zahorec *et al.* (2021), and explained as a tailings-filled surficial collapse up to 7 m thick with a density contrast of -300 kg/m^3 . From historical photographs and external evidence, we know that the surface collapses were back-filled with tailings. However, due to the character of our Growth solution source body A it seems that the back-filled surficial depressions cannot fully explain the gravity low A. Instead, our Growth solutions favour, in addition to the surficial back-fill, the presence of a negative contrast deeper source body respective to the pronounced gravity low. At the moment, its existence remains only a working hypothesis to be verified.

The depth weighting introduces another level of ambiguity into the purely gravimetric inversion. Unless controlled by independent constraining information, the level of ambiguity cannot be reduced. The drilling data are available only outside of the alleged body A and the boreholes reach only 30 m below surface. Currently, we have no other geophysical data to probe for the existence, nature and depth reach of the suspected deep source body A.

4. Discussion

From the description of the Growth inversion methodology (Camacho *et al.*, 2021b, 2024), as well as from our own experience with using the GROWTH-dg and GROWTH-23 tools, it stems that the Growth solutions with relatively small balance factor (λ) values represent over-fitting solutions (with too tight data fit in terms of misfit r.m.s.) that are contaminated with arti-

facts (model noise). On the other side, the Growth solutions with relatively high λ values represent over-compacted solutions (with poor fit in terms of misfit r.m.s.) that produce too rounded model source bodies that are shifted toward deeper positions. For that sake it is recommended to run several Growth inversions while sensibly varying the λ value while observing the behaviour of the model characteristics and the course of the misfit. If justifiable external expectations exist, such as borehole data, models resulting from interpretation using other geophysical methods and data, these may assist the above-described trial and error process of selecting the proper balance factor for the inversion.

It is known, and learnt from experience also, that the Growth solutions with small end condition values (% of filled cells of the subsurface partition) produce model source bodies that are too slim and of higher density contrasts. On the other hand, the Growth solutions with relatively high end-condition values (%) produce model source bodies that are too voluminous (overgrown) and have relatively small density contrasts. If the target density contrast of the solution can be argued out or reasonably expected, this will facilitate arriving at a model with properly voluminous source bodies.

It is known from experience that in case of gravity data generated by surficial or shallow flat horizontally extensive sources, the gravimetric inversion tends to produce horse-shoe shaped or empty-bowl shape source bodies pushed to deeper locations. This tendency can be in the Growth inversion suppressed or counter-acted by using the depth weighting, aka upward forcing (inversion parameter D). Again, the value of parameter D should be sensibly varied in a trial-and-error approach of repeating the inversion runs. External cognition, such as borehole data, is necessary to fix the proper value of parameter D.

With respect to the Čáry case study, it turned out that this is a very complex and difficult to handle by Growth inversion case. Also, the coverage of the study area by observed gravity data introduced additional challenges into the inversion problem. Tight-fit and overfitting Growth solutions indicated the presence of void space or partly filled space just above the depth level of the corridors and clearly associated with these mining access corridors, as demonstrated by the linear alignments parallel with the corridors. Such finding is partly obscured by the too coarse resolution of the Growth

models at the level of subsurface cell size of 8 m. In the future we plan to re-code and re-compile the Growth tools as to be able to handle smaller cell sizes at the level of 1 or 2 m, which should yield a more accurate image of the void space associated with the corridors.

A difficult to explain deeper body of negative density contrast (“A”), related to the pronounced gravity low in the NW sector of the data area, was indicated by the Growth inversion. From a range of admissible Growth models with no depth weighting (no upward forcing), it was inferred that this body reaches a depth of 40 to even 60 m below surface. Experimenting with the strength of upward forcing the depth reach of this body was lowered to some 20 m below surface, but never shallower than the horizon of the access corridors. By stripping the input gravity data for the effect of the surficial back-fill, this body could be recovered as less significant and of lower depth reach.

By analysing the whole range of admissible Growth models, the interpretation that the pronounced gravity low is produced solely by a surficial body such a back-filled surface depression due to surface subsidence/collapse is challenged. Since the bottom boundary of source body “A” reaches depths below the horizon of the corridors in the whole range of Growth solutions, it is very unlikely that it is just due to void or filled-up space. This leaves us with a hypothesis that this source body of a relatively high negative density contrast is of a structural geological origin. Such working hypothesis remains to be verified by exploration based on additional geophysical methods.

5. Conclusions

The Čáry case study demonstrated that the use of the Growth inversion can be beneficial in near surface microgravimetric exploration aimed at detecting void space such as in sinkhole hazard mitigation studies. By revisiting the Čáry gravity dataset and inverting the data by the Growth approach, we have detected the potentially ongoing sinkhole threat associated with the mining access corridors. We have also found a mysterious unexplained deeper body of negative density contrast related to the pronounced gravity low in the NW sector of the data area, yet to be confirmed and characterized by additional geophysical methods.

Acknowledgements. J.F. and J.B. were supported by Spanish Agencia Estatal de Investigación (10.13039/501100011033) grant G2HOTSPOTS (PID2021-122142OB-I00) and RADARQUIFER (MITECO 20233TE014). J.B. was supported also by the Doktorant grant system of the Slovak Academy of Sciences through the project No. APP0652. This work was partially supported also by the Slovak Research and Development Agency under the contract (project) No. APVV-19-0150 (acronym ALCABA), by the VEGA grant agency under projects No. 2/0002/23 and No. 1/0587/24.

References

- Bódi J., Vajda P., Pašteka R., Pánisová J., Papčo J., Zahorec P., Fernández J., 2025: Applicability of Growth inversion in microgravimetry for archeological prospection and sinkhole hazard detection: Jur, Koš and Senec case studies. *J. Appl. Geophys.*, **238**, 105718, doi: 10.1016/j.jappgeo.2025.105718.
- Camacho A. G., Prieto J. F., Aparicio A., Ancochea E., Fernández J., 2021a: Upgraded GROWTH 3.0 software for structural gravity inversion and application to El Hierro (Canary Islands). *Comput. Geosci.*, **150**, 104720, doi: 10.1016/j.cageo.2021.104720.
- Camacho A. G., Vajda P., Miller C. A., Fernández J., 2021b: A free-geometry geodynamic modelling of surface gravity changes using Growth-dg software. *Sci. Rep.*, **11**, 23442, doi: 10.1038/s41598-021-02769-z.
- Camacho A. G., Vajda P., Fernández J., 2024: GROWTH-23: An integrated code for inversion of complete Bouguer gravity anomaly or temporal gravity changes. *Comput. Geosci.*, **182**, 105495, doi: 10.1016/j.cageo.2023.105495.
- Čangel O., 2019: Detection of undermined territory by geophysical methods on the site Baňa Čáry, j.s.c., (Detekcia poddolaného územia geofyzikálnymi metódami na lokalite Baňa Čáry, a.s.). Diploma thesis, Comenius University, Bratislava, Slovakia (in Slovak).
- Vajda P., Bódi J., Camacho A. G., Fernández J., Pašteka R., Zahorec P., Papčo J., 2024: Gravimetric inversion based on model exploration with growing source bodies (Growth) in diverse earth science disciplines. *AIMS Math.*, **9**, 5, 11735–11761, doi: 10.3934/math.2024575.
- Zahorec P., Pašteka R., Papčo J., Putiška R., Mojzeš A., Kušnirák D., Plakinger M., 2021: Mapping hazardous cavities over collapsed coal mines: Case study experiences using the microgravity method. *Near Surf. Geophys.*, **19**, 3, 353–364, doi: 10.1002/nsg.12139.